Towards Substrate Engineering of Graphene-Silicon Schottky Diode Photodetectors

H. Selvi[1], N. Unsuree[1], E. Whittaker[1,3], M.P. Halsall[1,3], E.W. Hill[2,4], A. Thomas[3,5], P. Parkinson[3,6], and T.J. Echtermeyer[1,2,3*]

[1] *School of Electrical & Electronic Engineering, University of Manchester, Manchester M13 9PL, UK*

[2] *National Graphene Institute, University of Manchester, Manchester M13 9PL, UK*

[3] *Photon Science Institute, University of Manchester, Manchester M13 9PL, UK*

[4] *Manchester Centre For Mesoscience and Nanotechnology, University of Manchester, Manchester M13 9PL, UK*

[5] *School of Materials, University of Manchester, Manchester M13 9PL, UK and*

[6] *School of Physics and Astronomy, University of Manchester, Manchester M13 9PL, UK*

Supporting Information

I. X-RAY PHOTOELECTRON SPECTROSCOPY (XPS)

Fig.1 shows an XPS survey spectrum recorded from graphene on a silicon wafer with a native oxide film. The survey spectrum shows the presence of only carbon (C), Oxygen (O) and silicon (Si) indicating no contamination of the graphene and the native oxide. The peaks to the higher binding energy side of the Si 2s and Si 2p are due to plasmon satellites [1]. All spectra are aligned on the binding energy scale to the graphene C 1s peak at 285 eV [2].

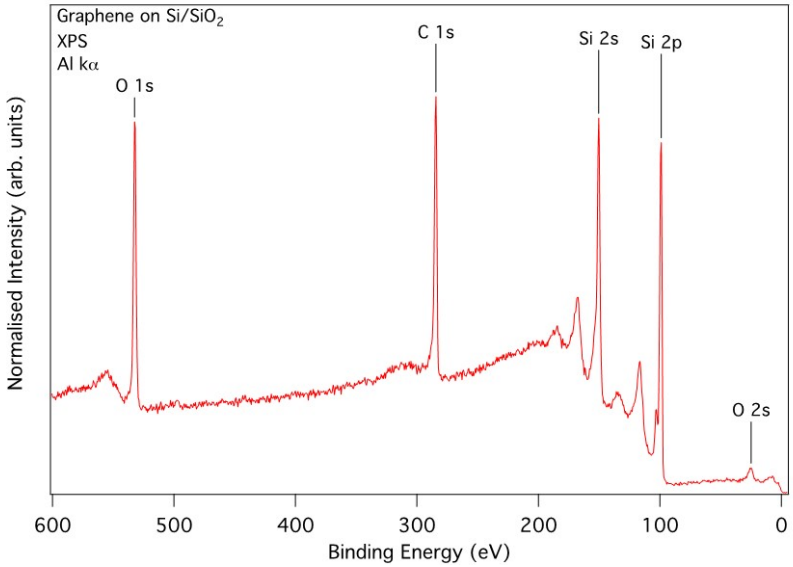

FIG. 1: XPS survey spectrum recorded from graphene on a silicon wafer with a native oxide film recorded at a pass energy of 160 eV at normal emission.

*Electronic address: tim.echtermeyer@manchester.ac.uk

Fig.2 shows a high-resolution spectrum of the C 1s core level, fitted with three peaks at binding energies of 285 eV, 286.6 eV and 289.5 eV, which are assigned to the graphene film and C-OH and C=O respectively. These most likely arise from traces of PMMA used in the transfer process, but may also be due to the presence of adsorbed atmospheric hydrocarbons. The graphene peak clearly dominates the spectrum. The asymmetry to the high binding energy is the expected Doniach-Sunjic line shape associated with conducting materials.

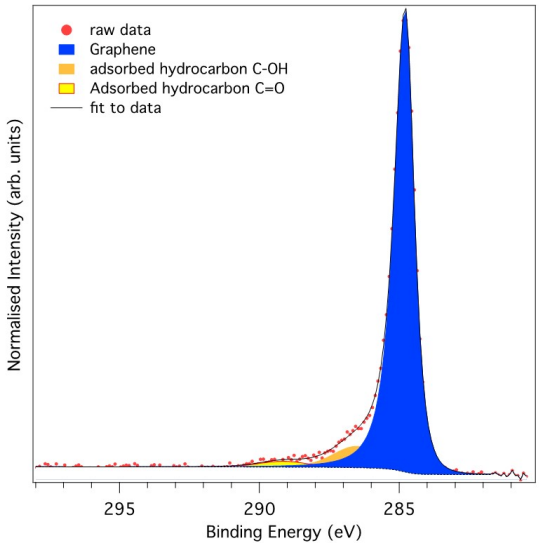

FIG. 2: High resolution C 1s spectrum recorded from graphene on a silicon wafer with a native oxide film. The spectrum was recorded at a pass energy of 20 eV.

II. OPTO-ELECTRONIC CHARACTERISATION

All electrical measurements were conducted in ambient atmosphere at room temperature apart from the temperature dependent measurements. The current-voltage (IV) measurements were performed using a computer-interfaced Keithley 2400 source-meter. As convention, the bias voltage is applied to the silicon substrate and graphene is grounded in all measurements. Laser diodes of wavelength $\lambda = 532$, 650 and 980 nm as well a monochromator (Spex 500M) with white light source (Thorlabs OSL1EC) were used to record the spectral response of devices under illumination. Neutral density (ND) filters were used to vary the light intensity. A beam splitter was inserted into the optical path to measure the power of the incident light (Thorlabs 120C). The high photoresponsivity of the diodes from near UV to IR allowed performing measurements at DC without need for a lock-in amplifier. High speed measurements were carried out using a pulsed laser ($\lambda = 405$nm) with a pulse width of 80ps and variable repetition rate and the electrical response recorded using a pre-amplifier (Zurich Instruments HF2TA) and an oscilloscope (WaveJet 354-A). LEDs of different wavelengths were modulated with a sine wave input signal using a signal generator in the frequency range up to hundreds of kHz.

III. RAMAN CHARACTERIZATION

The Raman spectrum of graphene on silicon (fig.3) was collected using a 514nm laser with a power less than 0.2 mW. The G peak position is 1592 cm^{-1} with a full width half maximum (FWHM) of 15 cm^{-1} and the 2D peak position is 2688 cm^{-1} with a FWHM 29 cm^{-1}. The FWHM of the 2D peak and 2D-to-G ratio

(~ 3.5) of the 2D peak indicate high quality monolayer graphene [3]. A small D peak observed at 1346 cm^{-1} is indicative of the presence of a small amount of defects, presumably due to CVD-graphene transfer.

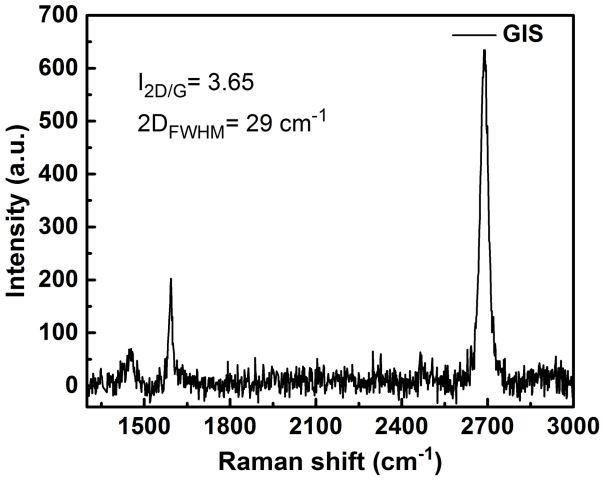

FIG. 3: Raman spectrum of graphene located on silicon surface in the GIS diode.

IV. I-V AND C-V CHARACTERISATION

Experimentally observed I-V curves can be described by the diode equation [4].

$$I = I_0[exp(\frac{q(V - IR_S)}{nk_BT}) - 1] \tag{1}$$

with

$$I_0 = AA^*T^2exp(\frac{-q\phi_B}{k_BT}) \tag{2}$$

V is the applied bias voltage, R_S is the series resistance of the diode, n is the diode ideality factor, k_B is the Boltzmann constant, q the electron charge, and T is the temperature in Kelvin. I_0 is known as saturation current or leakage current in the reverse bias, where, A is the Schottky diode contact area, A^* is the effective Richardson constant ($112A^{-2}K^{-2}$ for n-type silicon) and ϕ_B is the Schottky barrier height (SBH) for a given voltage.

The Schottky barrier height (SBH) ϕ_B can be calculated from eq.1 as

$$\phi_B = \frac{k_BT}{q}ln(\frac{AA^*T^2}{I_0}) \tag{3}$$

and ϕ_B can be quantitatively determined through temperature dependent I-V characterisation of the diode. The semi-logarithmic plot of I_0/T^2 vs. $1/k_BT$ in reverse operation bias at a particular reverse biases allows determination of the SBH (fig.4).

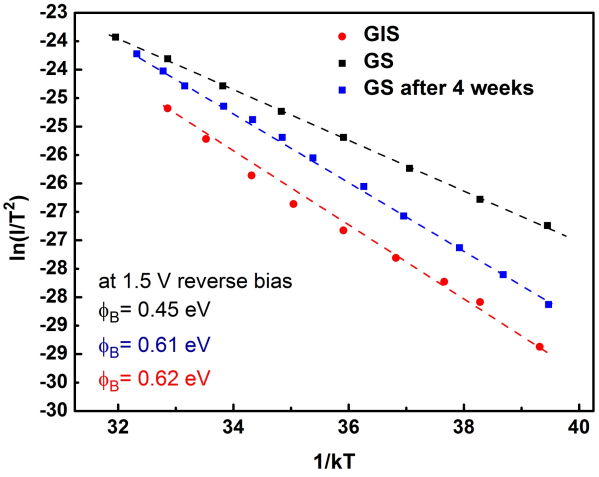

FIG. 4: Temperature dependent characterisation of the GIS and GS diodes. The GIS and GS diodes have an initial barrier height of 0.62 and 0.45 eV. The barrier height of the GS diode increases to 0.61 eV after four weeks of storage in ambient atmosphere due to the regrowth of the interfacial oxide layer in the junction.

Series resistance (R_S) and ideality factor (n) in eq.1 can be determined from the forward biased current-voltage characteristics using Cheungs function [5]:

$$\frac{dV}{dlnI} = n\frac{k_BT}{q} + IR_S \tag{4}$$

According to eq.4, the $dV/dlnI$ vs. I plot (fig.5) produces a straight line and its slope gives series resistance (R_S) and intercept on the vertical axis nk_BT/q. The ideality factor n of the diode is extracted in the linear

region of the I-V curve (0.3 - 1 V) as in [6]. We would like to point out that Cheung's method is extremely sensitive to the bias voltage range where it is applied. For example, comparing the I-V characteristics of the GS and GIS devices, the GS device exhibits a sharper increase in current in the low forward bias range (0 - 0.25 V). This results in unrealistic ideality factor values for the GS device of less than one. However, the forward current of the GIS device exhibits a higher slope in the linear region (0.3 - 0.7 V) compared to the GS device therefore has a lower ideality factor value. In this regard, in contrast to conventional MIS diodes where the existence of an oxide layer deteriorates the ideality factor [7–9], we observed a decrease of the ideality factor in the GIS diode with the interfacial oxide layer similar to an earlier report [10].

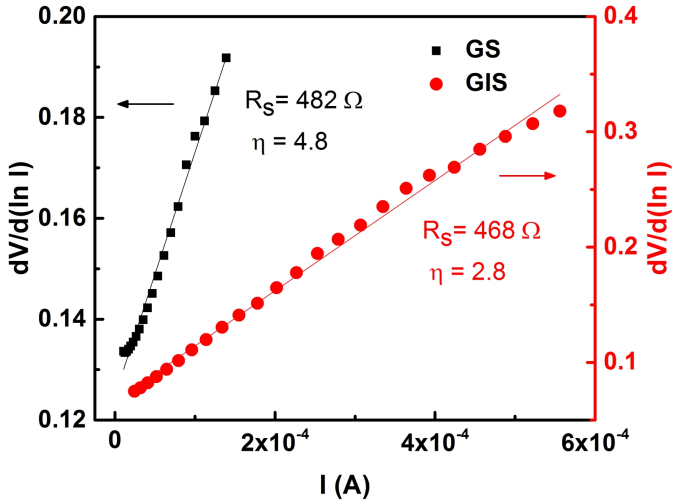

FIG. 5: GS device has an ideality factor of 4.8 however in the case of GIS device the ideality factor is improved to 2.8. Devices have similar series resistance values R_S of ≈ 0.5 kΩ.

Furthermore, additional characteristics of a Schottky diode such as doping density (N_d) of the substrate and built in potential (V_{bi}) of the junction can be determined from the slope of the Mott-Schottky plot (fig.6) [11, 12] using the relationship between capacitance and voltage given by

$$\frac{1}{C^2} = \frac{2(V_{bi} + V)}{qN_d\epsilon_0\epsilon_{Si}A^2} \tag{5}$$

where, A is the active area of the diode which is the Si-Gr interface, ϵ_0 is the permittivity of free space, ϵ_{Si} is the permittivity of silicon, N_d is the doping density of silicon, V is the applied reverse voltage and V_{bi} is the built-in voltage at the silicon surface. Plotting $1/C^2$ vs. V yields a straight line with slope $2/qN_d\epsilon_0\epsilon_{Si}A^2$and the intercept on the voltage axis is given by V_{bi}.

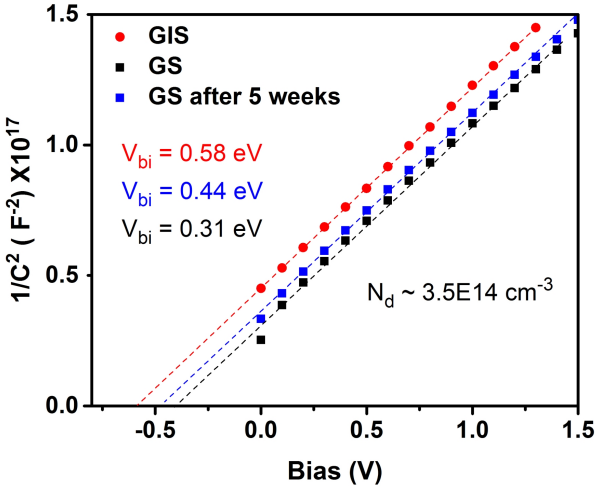

FIG. 6: $1/C^2$-V characteristics of the diodes under reverse bias at 1kHz frequency. The built-in voltage $V_{\rm bi}$ is 0.58 V and 0.31 V, for the GIS and GS diodes, respectively. In the GS device, the built-in voltage increases to 0.44 V after 5 weeks time due to the regrowth of interfacial oxide layer at the junction.

[1] Moulder, J.F., Stickle, W.F., Sobol, P.E., Bomben, K.D., *Handbook of X-ray Photoelectron Spectroscopy*, Perkin-Elmer Corp, Eden Prairie, MN, 1992

[2] Yang, D., et. al., Carbon **47**, 145 (2009)

[3] Ferrari, A.C., Meyer, J.C., Scardaci, V., Casiraghi, C., Lazzeri, M., Mauri, F., Piscanec, S., Jiang, D., Novoselov, K.S., Roth, S. and Geim, A.K., Physical review letters, **97** 187401 (2006)

[4] Sze, S.M. and Ng, K.K. *Physics of semiconductor devices* John wiley & sons, 2007.

[5] Cheung, S.K. and Cheung, N.W., Applied Physics Letters **49**, 85-87 (1986)

[6] Di Bartolomeo, A., Luongo, G., Giubileo, F., Funicello, N., Niu, G., Schroeder, T., Lisker, M. and Lupina, G., 2D Materials **4**, 025075 (2017)

[7] Card, H.C. and Rhoderick, E.H., Journal of Physics D: Applied Physics **4**, 1589 (1971)

[8] Card, H.C., Solid-State Electronics **20**, 971-976 (1977)

[9] Lillington, D.R. and Townsend, W.G., Applied Physics Letters textbf28, 97-98 (1976)

[10] Song, Y., Li, X., Mackin, C., Zhang, X., Fang, W., Palacios, T., Zhu, H. and Kong, J., Nano letters **15**, 2104-2110 (2015)

[11] Goodman, A.M., Journal of applied physics **34**, 329-338 (1963)

[12] Tyagi, M.S. Physics of Schottky barrier junctions. *In metal-semiconductor Schottky barrier junctions and their Applications*, Springer US, 1-60 (1984)